NMR structure of an anti-gp120 antibody complex with a V3 peptide reveals a surface important for co-receptor binding

Vitali Tugarinov[1], Anat Zvi[1], Rina Levy[1], Yehezkiel Hayek[1], Shuzo Matsushita[2] and Jacob Anglister[1]*

Background: The protein 0.5β is a potent strain-specific human immunodeficiency virus type 1 (HIV-1) neutralizing antibody raised against the entire envelope glycoprotein (gp120) of the HIV-1_{IIIB} strain. The epitope recognized by 0.5β is located within the third hypervariable region (V3) of gp120. Recently, several HIV-1 V3 residues involved in co-receptor utilization and selection were identified.

Results: Virtually complete sidechain assignment of the variable fragment (Fv) of 0.5β in complex with the $V3_{IIIB}$ peptide P1053 (RKSIRIQRGPGRAFVTIG, in single-letter amino acid code) was accomplished and the combining site structure of 0.5β Fv complexed with P1053 was solved using multidimensional nuclear magnetic resonance (NMR). Five of the six complementarity determining regions (CDRs) of the antibody adopt standard canonical conformations, whereas CDR3 of the heavy chain assumes an unexpected fold. The epitope recognized by 0.5β encompasses 14 of the 18 P1053 residues. The bound peptide assumes a β-hairpin conformation with a QRGPGR loop located at the very center of the binding pocket. The Fv and peptide surface areas buried upon binding are 601 Å and 743 $Å^2$, respectively, in the 0.5β Fv–P1053 mean structure. The surface of P1053 interacting with the antibody is more extensive and the V3 peptide orientation in the binding site is significantly different compared with those derived from the crystal structures of a V3 peptide of the HIV-1 MN strain ($V3_{MN}$) complexed to three different anti-peptide antibodies.

Conclusions: The surface of P1053 that is in contact with the anti-protein antibody 0.5β is likely to correspond to a solvent-exposed region in the native gp120 molecule. Some residues of this region of gp120 are involved in co-receptor binding, and in discrimination between different chemokine receptors utilized by the protein. Several highly variable residues in the V3 loop limit the specificity of the 0.5β antibody, helping the virus to escape from the immune system. The highly conserved GPG sequence might have a role in maintaining the β-hairpin conformation of the V3 loop despite insertions, deletions and mutations in the flanking regions.

Addresses: [1]Department of Structural Biology, The Weizmann Institute of Science, Rehovot 76100, Israel and [2]Center for AIDS Research, Kumamoto University Medical School, Honjo1-1-1, Kumamoto 860-8556, Japan.

*Corresponding author.
E-mail: bpanglis@weizmann.ac.il

Key words: anti-gp120 antibody, co-receptor, HIV-1, NMR, V3 loop

Received: **14 December 1999**
Revisions requested: **29 January 2000**
Revisions received: **11 February 2000**
Accepted: **16 February 2000**

Published: **24 March 2000**

Structure 2000, **8**:385–395

0969-2126/00/$ – see front matter

Introduction

The binding of human immunodeficiency virus type 1 (HIV-1) to its target cells is mediated by the envelope glycoprotein of the virus, gp120. Initially, gp120 binds to CD4, a molecule found on the surface of both T cells and macrophages, triggering conformational changes in gp120 that expose a binding site to either CCR5 or CXCR4 chemokine receptors. The virus infects the target cell only after binding to one of these co-receptors and the HIV-1 phenotype is determined by the chemokine receptor it recognizes. Macrophage-tropic strains use CCR5 for fusion and entry into the target cell and are designated R5 viruses [1]. They are slow-replicating, non-syncytium-inducing and are less sensitive to neutralization by soluble CD4 and anti-V3 (V3, third hypervariable region of gp120) antibodies than T-cell tropic strains. T-cell tropic strains use CXCR4 (fusin) as a co-receptor [2–7] and are designated X4 viruses. X4 viruses are fast-replicating, syncytium inducing and sensitive to neutralization by soluble CD4 and by anti-V3 antibodies. Dual tropic viruses use both CXCR4 and CCR5 and are designated R5X4 viruses.

Genetic analyses of the HIV-1 genome have demonstrated that V3 contains major determinants responsible for the phenotype of the virus and cell tropism. HIV-neutralizing antibodies against V3 do not inhibit gp120 binding to CD4; however, they prevent fusion of the virus with its target cell [8]. Recent experiments have shown that human anti-V3 antibodies inhibit the binding of the R5 gp120–CD4 complex to CCR5 co-receptor [9,10].

Exchange of V3 from the IIIB strain (an X4 virus) with V3 of an R5 virus renders the virus infection susceptible to inhibition by chemokines specific to CCR5 [11].

A cyclic V3 peptide corresponding to the complete V3 loop of an R5 virus binds to the membranes of monocyte-derived macrophages at sub micromolar concentrations [12]. The proteins involved in the binding were identified as CCR5 and CD4, and it has been suggested that V3 forms a ternary complex with these two proteins [12]. Indeed, CD4 and CCR5 were found to be associated in a 3T3 cell line transfected to express CD4 and CCR5 and this association is independent of gp120 or any other ligand [13]. Cyclic V3 peptides of X4 viruses were found to inhibit in a dose-dependent manner both antibody binding to CXCR4 and infection by X4 viruses [14], providing evidence that cyclic V3 can interact with CXCR4 independently of other gp120 domains. Concentrations of cyclic V3 peptides as low as 1–5 μM caused 50% inhibition of HIV-1 infection [14]. Linear V3 peptides corresponding to R5 and X4 viruses inhibit infection of $CD4^+$ HeLa cells expressing either CCR5 or CXCR4 or both [15]. All these experiments demonstrate clearly that V3 interacts directly with CCR5 and CXCR4 and is a significant component of the gp120 interface involved in co-receptor binding. High-affinity binding of gp120 to the chemokine receptors, however, requires participation of other domains in gp120 such as the CD4i epitope [16].

Most neutralizing antibodies against HIV in infected individuals are directed against V3 [8]. Therefore, V3 has been regarded as the principal neutralizing determinant (PND) of HIV-1. Experimental data from different laboratories, however, have shown that anti-V3 antibodies are not important for the neutralization of R5 viruses [17–19]. This could be explained if the V3 loop of R5 viruses is occluded in dormant viruses and become exposed for a short period of time only after CD4 binding. Steric hindrance might prevent antibody binding to V3 once the virus is bound to CD4.

Three anti-V3 peptide antibodies in complex with HIV-1 MN strain ($HIV\text{-}1_{MN}$) peptides were studied using X-ray crystallography [20–22]. These antibodies recognized small epitopes thus preventing the determination of the V3 global conformation. Moreover, the V3 loop peptide was found to have different conformations in complexes with different anti-peptide antibodies [22]. The structure of the gp120 core in complex with a CD4 fragment and an HIV-neutralizing antibody has been solved recently using X-ray crystallography [23]. To enable crystallization, however, the variable loops of gp120, including V3, were truncated and the carbohydrates were removed [23]. The 0.5β antibody used in the present study is a potent strain-specific HIV-neutralizing antibody [24] raised against the entire gp120 of the $HIV\text{-}1_{IIIB}$ strain. Neutralization of the free virus is obtained at 0.5β concentration of 100 ng/ml, and full neutralization of infected cells, as measured by syncytium inhibition, is achieved at antibody concentrations as low as 50 μg/ml [24]. The antibody 0.5β recognizes the 24-residue PND peptide RP135 (NNTRKSIRIQRGPGRAFVTIGKIG, in single-letter amino acid code) and the whole gp120 with comparable affinities of 2×10^8 M^{-1} and 7×10^7 M^{-1}, respectively [25]. Our previous ^1H nuclear magnetic resonance (NMR) and binding studies of the 0.5β–RP135 peptide complex defined the boundaries of the determinant recognized by the antibody as Lys^{5P}–Ile^{20P} (where P denotes peptide) of RP135 [26,27]. The V3 peptide P1053 (RKSIRIQRGPGRAFVTIG; the peptide residues are numbered as Arg^{4P} through Gly^{21P} according to RP135) comprises the complete 0.5β epitope and binds to the antibody with almost the same affinity as RP135 [27]. The conformation of P1053 in complex with 0.5β was determined using nuclear Overhauser effect spectroscopy (NOESY) difference spectra with the 0.5β antigen-binding fragment (Fab) [28] and by isotope-filtering experiments with uniformly ^{15}N- and ^{13}C-labeled ([U–^{15}N,^{13}C]) Fv [29]. The structure of the 0.5β-bound P1053 peptide consists of two antiparallel strands linked by a QRGPGR loop with a *cis*-proline type VI RGPG turn [29]. Most recently, we proposed a model of the 0.5β–P1053 complex [30]. The peptide was docked into the modeled antibody combining site on the basis of seven intermolecular NOEs and one 'mutant cycle' distance restraint, and could be only approximately located in the 0.5β binding site [30]. Unambiguous assignments of the interacting tyrosine residues of the antibody were not possible [30], thus preventing us from addressing several structurally important issues.

The Fv is the smallest antigen-binding fragment of antibody molecules. It consists of the non-covalently associated variable domains of the light (VL) and heavy (VH) chains, and contains six hypervariable complementarity determining regions (CDRs) that form the antibody binding site (L1, L2 and L3 are the CDRs of the light chain and H1, H2 and H3 are the CDRs of the heavy chain). The core of each domain consists of a highly conserved framework, which forms the immunoglobulin fold. Each of the CDRs excluding H3 folds into a restricted number of canonical conformations classified based on the crystal structures of numerous antibodies [31,32]. The Fv fragments generally retain the specificity and affinity of the parent antibody [33]. The molecular weight of the Fv (~25 kDa) is half that of the Fab fragment and it is by far more suitable for detailed NMR investigations. Here, we describe the well-resolved solution structure of the binding site of 0.5β Fv in complex with the V3 peptide P1053. Possible implications of the V3 structure and its solvent accessibility in gp120 for co-receptor binding and the anti-V3 humoral immune response are discussed.

To the best of our knowledge, this is the first antibody–peptide binding-site structure that has been determined entirely from NMR restraints.

Results and discussion

0.5β Fv sidechain assignments and NOE interactions

The backbone and C^{β} resonance assignments of the complexed form of 0.5β Fv were reported earlier [34]. In this study, the assignment of aliphatic sidechains was achieved by the combined use of triple-resonance and ^{13}C-edited NMR spectroscopy. The final extent of assignments was 98.7% for the Fv backbone (excluding proline ^{15}N) and 92.6% for the Fv aliphatic sidechains (excluding labile ^{15}N-bound sidechain protons). The combining site of the complex is exceptionally rich in aromatic residues with eight tyrosines, two histidines, a phenylalanine and a tryptophan, all located at or near the Fv–peptide interface. The ^{13}C and ^{1}H spin connectivities within the aromatic rings were established using TROSY (transverse relaxation-optimized spectroscopy) experiments [35,36], and the aromatic resonances were subsequently assigned to specific residues using the Cβ(Cγ)CδHδ experiment [37]. The residues Tyr^{32L}, Tyr^{91H}, Phe^{62L} and His^{76L} did not provide C^{β}–H^{δ} connectivities and were assigned using (H)CCH-TROSY [36] and NOE connectivities in the ^{13}C-separated NOESY spectra (the position of an amino acid residue in the Fv sequence [31] is indicated by the standard three-letter abbreviation followed by a number and capital letter in superscript: L or H denoting light or heavy chain residue, respectively). Dramatically improved signal-to-noise ratios and narrower carbon line widths of the slowly relaxing TROSY [35,36] component enabled us to assign the sidechains of all 16 Fv tyrosines. The aromatic region of the ^{1}H-^{13}C TROSY [36] spectrum of the 0.5β Fv complexed with the unlabeled P1053 is shown in Figure 1. The resonance assignments of the aromatic sidechains were verified using ^{13}C-edited NOESY experiments. Strong NOEs between $H^{\delta}(C^{\delta})$ and the β-protons of the aromatic residues helped to complete the assignments based on J connectivities. The following aromatic resonances remain unassigned: $C^{\varepsilon}/H^{\varepsilon}$, C^{ζ}/H^{ζ} of Phe^{71L}, all the resonances of Phe^{98L}, $C^{\varepsilon}/H^{\varepsilon}$ and C^{ζ}/H^{ζ} of Phe^{29H}, and the imidazole resonances of His^{95H}.

The framework of the 0.5β light chain shares 96% sequence homology with that of the 50.1 antibody [20] light chain, whereas the heavy chain framework is 80% homologous to that of the HYHEL-5 antibody [38]. The long- and medium-range backbone NOEs detected in the ^{15}N- and ^{13}C-edited NOESY spectra of both Fv chains were examined against distances in the 0.5β model [27], rebuilt using the coordinates of 50.1 for the light chain [20]. The NOE and J-coupling data showed almost quantitative agreement with the distances and dihedral angles of the

Figure 1

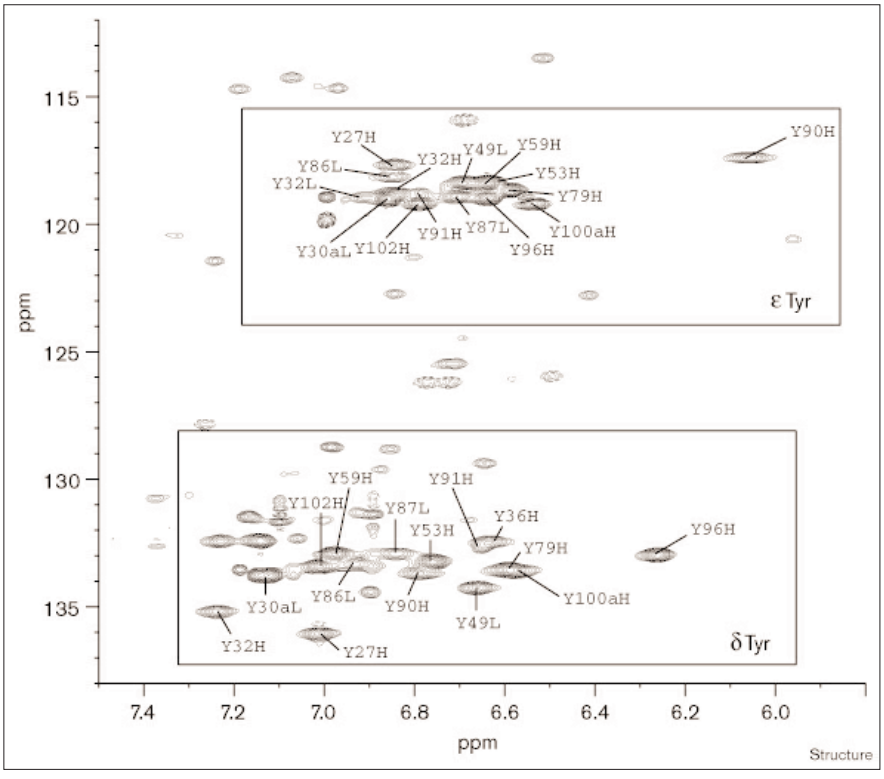

2D ^{1}H–^{13}C TROSY [36] 800 MHz spectrum of the 0.5β Fv complexed with the unlabeled P1053 peptide recorded in D_2O at 32°C (10 h total acquisition time). The assignments of the 0.5β Fv tyrosine residues are indicated. Negative peaks are shown with dashed contours and correspond to the resonances of the carbon nuclei bound to an uneven number of carbons ($C^{\delta 2}$ and $C^{\delta 1}$ of histidine and tryptophan rings, respectively). The cross-peaks of δ-Tyr^{32L} and ε-Tyr^{95H} are below the contour levels of the plot.

conserved part of the 0.5β model. For example, from 114 long- and medium-range intra-chain H^N–H^N, H^N–H^α and H^α–H^α contacts within a distance range of 3.5 Å that exist in the framework region of 0.5β model, 98 were identified as medium-to-strong cross-peaks in the NOESY spectra. The remaining 16 cross-peaks could not be detected because of overlap and/or exchange broadening of amide resonances. The NMR data were used, therefore, to calculate the structure of the Fv CDRs in complex with P1053, assuming that the 0.5β model represents the structure of the Fv framework with sufficient accuracy.

The intermolecular Fv–P1053 contacts were identified using a combination of two approaches. Where possible, these NOEs could be assigned using ^{13}C- and/or ^{15}N-filtering in one of the spectral dimensions [29]. Unfortunately, only ~75–80% isotopic labeling was achieved in the Fv samples used for these measurements, seriously compromising the quality of the filtered spectra. Many of the peptide protons interacting with the antibody belong to unlabeled methyl groups with favorable transverse relaxation properties. We found it advantageous to substitute the ^1H evolution period in the isotope-edited NOESY spectra by either constant-time or semi-constant time evolution periods very similar to the well-known BIRD (bilinear rotation decoupling) module [39] (see the Materials and methods section). This resulted in sign inversion of all those NOEs originating from ^{12}C-bound (P1053) protons as shown in Figure 2. The observed intermolecular NOEs between the 0.5β Fv CDRs and P1053 are summarized in Tables 1 and 2. The Fv heavy chain interacts through hydrophobic and polar sidechains. H1 and H2 make the most significant contribution to the interactions with the peptide. Thr^{31H} γ-methyl and the aromatic rings of His^{52H} and Tyr^{53H} interact extensively with the hydrophobic sidechains of both β strands of P1053. Unlike other antibody–ligand complexes solved using X-ray crystallography, the H3 residues of 0.5β provide only a small fraction of the antibody–ligand contacts. Except for Asn^{92L}, all the light chain residues interacting with the peptide are hydrophobic (Tyr^{30aL} [for the CDR numbering nomenclature see Table 1], Tyr^{32L} and Phe^{96L}). No NOE interactions between L2 and P1053 were observed. The P1053 epitope consists of residues from Lys^{5P} to Phe^{17P} and the sidechain of Ile^{20P}. Ile^{7P}, *cis*-Pro^{13P} and Gly^{14P} provide the most significant contribution to the observed peptide–antibody NOE contacts. Interestingly, these are the most conserved V3 loop residues among different HIV-1 strains [40].

Figure 2

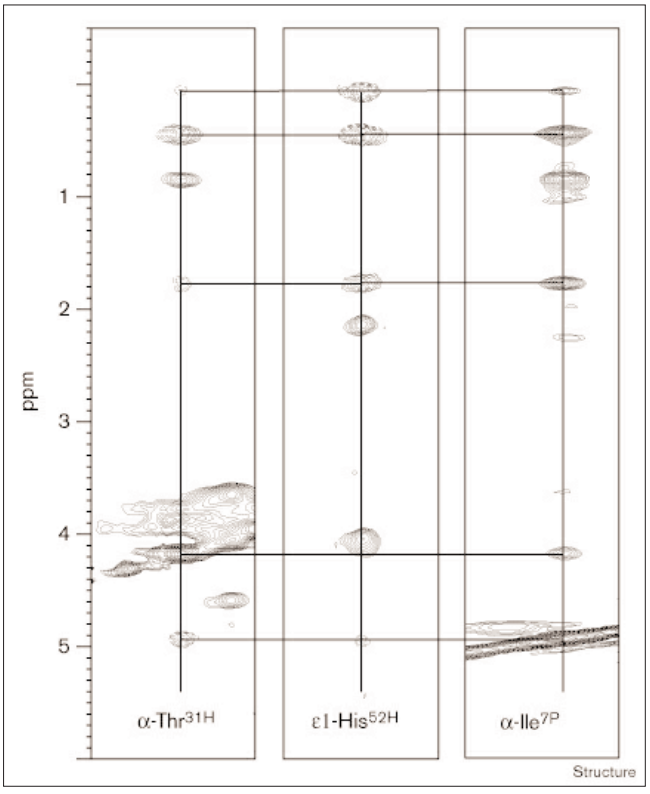

^1H–^1H strip plots of the F2-filtered ^{13}C-NOESY spectrum (right panel), the ^{13}C-edited NOESY with the BIRD [39] t1 evolution period (central and left panels) drawn at the frequencies of α-Thr^{31H}, ε1-His^{52H} and α-Ile^{7P} resonances and showing NOE interactions with Ile^{7P}. The F2-filtered ^{13}C-NOESY spectrum features both intra-peptide and Fv–peptide NOEs. Negative peaks are shown with dashed contours and correspond to the Fv–peptide intermolecular NOEs in the 'BIRD-supplemented' spectra.

The structure of the 0.5β binding site in complex with P1053

The structure calculations were carried out with 1138 distance and 80 dihedral restraints for P1053 and those Fv residues permitted to move (see Materials and methods section). Structural statistics for 40 structures of the 0.5β

Table 1

0.5β CDR canonical structures and the Fv–P1053 NOE contacts*.

CDR†	Sequence	Canonical structure (κ)
L1	24 KASQSVD***Y***DGDS***Y***MN 34 (30 30a 30d 32)	5
L2	50 AASNLES 56	1
L3	89 QQS***N***EDP***F***T 97	1
H1	26 GYTF***TTYP***IE 35	1
H2	50 NF***H***P***Y***SDDT***N***YNEKFKG 65 (52a 53)	2A
H3	95 HYGS***A***YAMDY 101 (99 100a)	'bulged'

*The CDR residues having NOE contacts with P1053 are shown in bold and italicised; †CDR numbering follows that of Al-Lazikani *et al.* [71].

Table 2

The Fv–P1053 NOE contacts*.

Peptide residues	Fv contact residues
Lys5	Tyr53 (H2)
Ser6	Thr31 (H2)
Ile7	Thr30 (H1), Thr31 (H1), His52 (H2), Tyr53 (H2), Ser54 (H2)
Arg8	His52 (H2)
Ile9	His52 (H2)
Gln10	Pro33 (H1), His52 (H2), Asn58 (H2)
Arg11	Asp56 (H2)†
Gly12	Phe96 (L3)
Pro13	Tyr30a (L1), Asn92 (L3), Phe96 (L3)
Gly14	Tyr32 (L1), Asn92 (L3), Phe96 (L3), Ala99 (H3)
Arg15	Ala99 (H3)
Ala16	Ala99 (H3)
Phe17	Thr31 (H1), Tyr32 (H1), Ala99 (H3)
Ile20	Tyr53 (H2)

*The P1053 residues having backbone–backbone NOE contacts with the Fv are shown in bold and italicised; †The Arg^{11P}–Asp^{56H} contact was inferred from earlier mutational studies (see text).

Table 3

Structural statistics for the set of 40 structures of the 0.5β Fv–P1053 binding site*.

Restraints and violations	
Intra-CDR medium and long-range restraints	442
Inter-CDR distance restraints	161
Intra-P1053 distance restraints†	201
Intermolecular Fv–P1053 distance restraints	92
P1053 dihedral restraints†	11
Fv CDR ϕ angle restraints	47
Fv CDR χ_1 angle restraints	22
Maximum individual NOE violation (Å)	0.34
Average rmsd of NOE violations (Å)	0.022 ± 0.003
Average rmsd of dihedral violations (°)	0.62 ± 0.112
Average rmsd from ideal covalent geometry	
Bond lengths (Å)	0.0026 ± 0.0002
Bond angles (°)	0.4800 ± 0.0223
Improper angles (°)	0.4375 ± 0.0348
Pair-wise rmsd values‡	
Backbone atoms (Å)	0.67 ± 0.12
All heavy atoms (Å)	1.44 ± 0.17
P1053 backbone atoms (Å)	0.92 ± 0.23
P1053 all heavy atoms (Å)	1.89 ± 0.36
P1053 K5-I7 and F17-I20 all heavy atoms (Å)	1.24 ± 0.32
P1053 RGPGR loop all heavy atoms (Å)	1.66 ± 0.60

*The reported structural statistics were calculated for the 0.5β Fv CDR and P1053 residues that were allowed to move during structure calculations (see the Materials and methods section). †Taken from [29] (see the Materials and methods section). ‡Calculated for the structures superimposed for the exact fit of the framework backbone atoms (see Figure 3).

binding site in complex with P1053 are presented in Table 3. The backbone stereoview of 0.5β Fv in complex with P1053 is shown in Figure 3. All Fv CDRs except H3 adopt standard canonical conformations (Table 1). The coordinates of the ensemble of NMR structures differ significantly (mean backbone root mean square deviation [rmsd] > 1.0 Å) from the 0.5β model [27] in L1, H1 and H3. The mean backbone rmsd values of the model versus the ensemble of NMR structures are 1.45 ± 0.12 Å, 1.06 ± 0.15 Å and 6.18 ± 0.05 Å for L1, H1 and H3, respectively. The same Fv CDRs have all heavy-atom displacements exceeding 2.0 Å (2.37 ± 0.21 Å, 2.58 ± 0.32 Å and 8.09 ± 0.09 Å for L1, H1 and H3, respectively) compared with the Fv model. In L1 and H1 the atomic displacements are predominantly local and concentrated at the flexible tip of the L1 β hairpin (Asp^{30bL}–Gly^{30cL}) and around the beginning of a helical turn in H1 (Tyr^{27H} and Thr^{28H}), whereas H3 revealed a totally different and unexpected fold.

H3 conformations were recently classified based on numerous antibody crystal structures [41]. According to the proposed rules [41], H3 in 0.5β should adopt a regular β-hairpin fold given that it has a neutral isoleucine residue at position 94H (usually occupied by arginine or lysine that form salt bridges with aspartic acid at position 101H). Nevertheless, the 0.5β H3 has a 'bulged torso' [41] conformation with a bulge at Asp^{101H} as manifested by many characteristic NOE contacts. The two antiparallel strands of H3 are linked by a YGSAYA multiple-turn loop. This fold enables a tight packing of hydrophobic sidechains. The Tyr^{96H} (H3) ring is packed against the ring of Tyr^{32H} (H2) and the sidechains of Ile^{94H} and Tyr^{102H} (both H3), whereas the ring of Tyr^{100aH} (H3) is packed against Tyr^{49L} (N-terminal to L2) as shown in Figure 4a. This packing resembles the usually encountered conformation of 'bulged torso' H3 hairpins [41]. As a result of this packing, Ala^{99H} (H3) interacts with the bound peptide. The binding site of 0.5β contains a contiguous hydrophobic surface consisting of the sidechains of aromatic residues (Figure 4a), alanine and proline. The bottom of the binding pocket is located at the interface between the Fv light and heavy chains and is comprised of Phe^{96L}, Trp^{47H} and Glu^{35H} sidechains. His^{95H} and Ala^{99H} form a rim on the right side of the pocket limiting the space available for the peptide.

The sidechains of both β strands of P1053 are in contact with H1, H2 and the H1–H2 interface (Figure 4a). The GPG segment of P1053 is buried deeply at the center of the binding pocket, with Pro^{13P} interacting with the aromatic rings of Tyr^{30aL} and Phe^{96L}. The amide of Gly^{14P} most probably forms an intermolecular hydrogen bond with the carbonyl of Ser^{95L} (L3). The type VI RGPG turn ensures a sharp reversal in the direction of the polypeptide chain so that both preceding and succeeding residues of the compact β hairpin of P1053 can interact with the antibody. The GPG segment of P1053 is sandwiched between the aromatic rings of Tyr^{30aL}, Tyr^{32L} (both L1), Phe^{96L} (L3) and Tyr^{100aH} (H3), and its conformation seems to be crucial for efficient binding.

The combining site of 0.5β contains several negatively charged sidechains, whereas the P1053 peptide contains

Figure 3

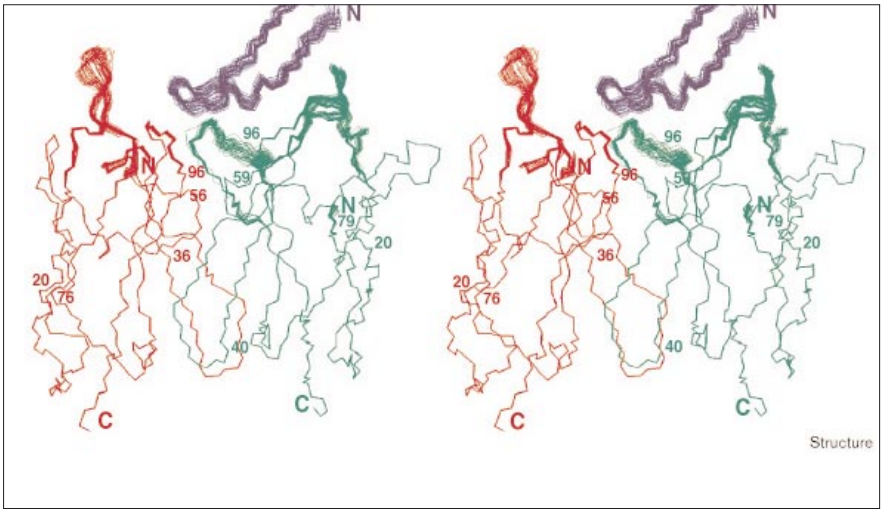

Stereoview superposition of 40 0.5β Fv–P1053 complex backbone structures. The Fv framework regions are superimposed exactly, as their coordinates were fixed during the structure calculations (see the Materials and methods section and text). The light and heavy chains of the Fv and the P1053 peptide are colored red, green and blue, respectively.

four arginines and one lysine. The binding of the Arg4→Lys and Arg11→Lys mutants of P1053 to 0.5β is comparable to that of the unmodified peptide [28]. The conservative Arg8→Lys, Arg8→His and Arg15→Lys mutations reduced the binding by more than two orders of magnitude [28] indicating that Arg^{8P} and Arg^{15P} sidechains are critical for interactions with 0.5β. Indeed, as shown in Figure 5 Arg^{8P} and Arg^{15P} form the largest contact areas with the antibody in the mean structure, whereas the sidechain of Arg^{11P} is among the most exposed to the solvent in the bound P1053. Arg^{4P} is completely outside the epitope recognized by 0.5β. The sidechain protons of Arg^{15P} and Arg^{8P} could not be definitely assigned from the isotope-filtered spectra [29]. Therefore, no NOE constraints were used for the sidechains of these residues. It was found that when the backbone dihedral restraints determined from solid-state NMR data [42] are used for Arg^{15P}, its sidechain invariably points towards and most probably forms a buried salt bridge with the carboxyl of Glu^{35H}. In the calculated structures, the methylene protons of Arg^{15P} interact extensively with the aromatic ring of Phe^{96L} (L3) and with the hydrophobic sidechains of Pro^{33H} (H2) and His^{95H} (H3) of 0.5β. The sidechain of Arg^{8P} is almost completely buried in the resulting structures. The methylene protons of Arg^{8P} have extensive intra-peptide interactions with the ring of Phe^{17P} and with the methylene protons of Arg^{15P}. The guanidinium group of Arg^{8P} approaches the surface close to the H1–H3 interface and could potentially interact through hydrogen bonds with the backbone carbonyl oxygens of Pro^{33H} (H2) and/or His^{95H} (H3). The structural reasons for the uncompensated and partially buried charge in the intermolecular interface are unclear. The existence of a previously postulated intermolecular Arg^{11P}–Asp^{56H} solvent-exposed salt-bridge [30] could not be directly corroborated by the present NMR data. The sidechain of Asp^{56H} is disordered

Figure 4

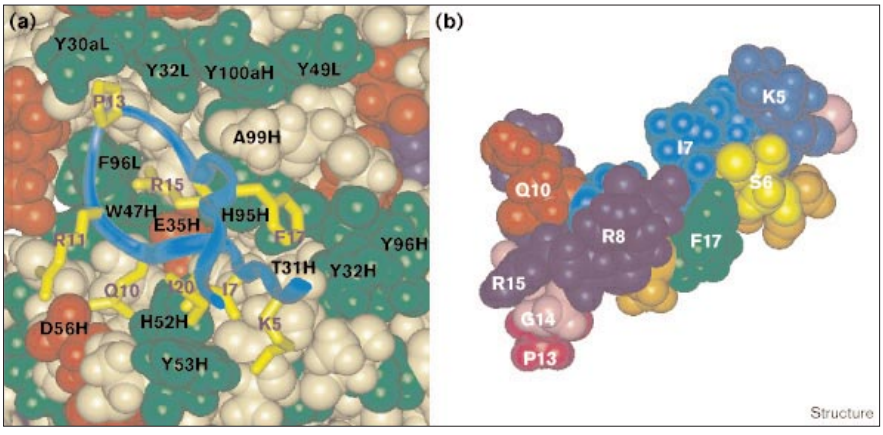

The structure of the 0.5β–P1053 binding interface. **(a)** A space-filling representation of the 0.5β binding site (mean 0.5β Fv–P1053 structure). The 0.5β residues are colored as follows: aromatic, green; acidic, red; and basic, blue. The bound P1053 peptide backbone is shown as a light blue ribbon. Several of the most extensively interacting sidechains of the peptide are shown in yellow and labeled in black. **(b)** The face of P1053 buried by the 0.5β antibody upon binding. The residues of the peptide in contact with the antibody and those spatially adjacent to them are labeled.

Figure 5

Surface characterization of the bound P1053 peptide. Black bars represent the solvent surface accessibility of the residues of bound P1053 (in % of the total van der Waals surface of the residue). Grey bars represent the relative contribution of each peptide residue to the Fv–P1053 contact surface area (in % of the total contact surface area contributed by the peptide).

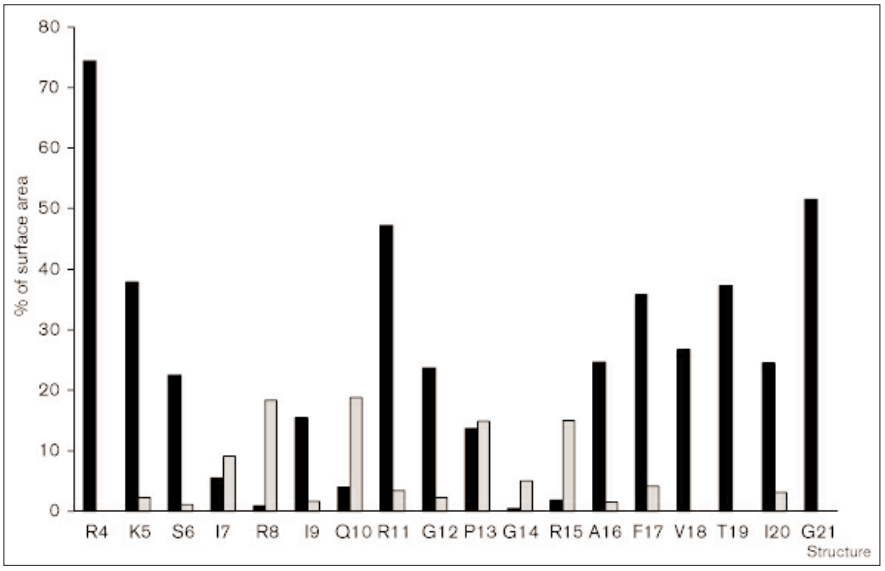

as judged by strong $^{3}J_{H\alpha H\beta}$ couplings to both of its β-protons. It is possible that the surface salt bridge is not thermodynamically stable and is destroyed at the slightly elevated temperatures used for NMR measurements. The sidechain of Arg^{11P} is in close proximity to the carboxyl of Asp^{56H}, however, and the distance constraint between them did not perturb the resulting structures.

The mean atomic displacements of the P1053 peptide in the 0.5β Fv–P1053 ensemble of structures versus the bound peptide in the averaged coordinates of the recently calculated Fab–P1053 model [30] are 8.60 ± 0.33 Å and 10.2 ± 0.43 Å for the backbone and all heavy atoms, respectively. These differences do not arise from different conformations of the peptide itself, however, given that the same intra-peptide restraints [30] were used in both studies. These differences rather represent a significant shift in the position of the bound P1053 compared with the proposed model, primarily because of an order-of-magnitude increase in unambiguously identified intermolecular contacts in the Fv–P1053 complex (5.1 versus 0.4 per peptide residue). Given that most of the intermolecular contacts involve the sidechain atoms of P1053, a significantly better definition of the bound peptide sidechains was achieved (Table 2). The more accurate positioning of the peptide within the 0.5β combining site structure and a significantly better definition of both the Fv CDRs and P1053 coordinates allowed us to address several biologically important issues concerning the V3 structure and function.

Anti-gp120 0.5β antibody versus antipeptide antibodies

The surface areas buried upon P1053 binding to the anti-gp120 0.5β antibody are 601 and 743 Å^2 for the 0.5β Fv and the P1053 peptide, respectively. The surface area contributed by 0.5β is therefore on average 13% and 28% larger than that contributed by the antipeptide antibodies 50.1 [20] and 59.1 [21], respectively, and is close to that reported for the antibody 58.2 [22]. The peptide contribution exceeds that of 50.1, 59.1 and 58.2 complexes by 56%, 73% and 29%, respectively. The P1053 interacting surface, consisting of all peptide residues except for Arg^{4P}, Val^{18P}, Thr^{19P} and Gly^{21P}, is more extensive than that observed in the X-ray studies of the complexes of $V3_{MN}$ peptides with antipeptide antibodies and is larger than the combination of the peptide epitopes recognized by 50.1 and 59.1 antipeptide Fabs [20,21]. The peptide orientations within the binding pocket also differ substantially. For example, P1053 interacts extensively with H1 and the H1–H2 interface (Table 2; Figure 4a), quite unlike the peptides studied using X-ray crystallography [20–22].

V3 peptides are flexible when they are free in solution and therefore antibodies raised against such peptides recognize different V3 conformations [22]. The conformation of V3 in native gp120 should be considerably more restricted. V3-directed antibodies raised against the entire envelope glycoprotein recognize the native V3 conformation and are able to induce this conformation in flexible V3 peptides. We cannot exclude the possibility that the loop at the tip of the β hairpin in gp120 exhibits some conformational flexibility. In this case 0.5β might select one out of a family of structures of this loop or even induce a different structure into the QRGPGR sequence in P1053. Nevertheless, our working model is based on the assumption that the V3 loop is structured in intact gp120 and manifests a similar structure when bound to the 0.5β antibody.

The V3 surface buried upon antibody binding

The peptide surface interacting with the antibody is depicted in Figure 4b. This side of the V3 loop is most likely to be exposed in the free gp120 that was used as an immunogen. As V3 is involved in the interaction of gp120 with the chemokine receptors found on T cells and macrophages, this exposed surface probably contains residues contributing to co-receptor binding. The V3 loops of M-tropic and T-tropic viruses share considerable sequence homology. A switch in the phenotype of the virus from syncytium-inducing to non-syncytium-inducing or vice versa was found to depend on the charge of the residues at positions 306 (Ser^{6P} in P1053), 320 and 324 [43]. The last two residues are absent from P1053. Later on, it was found that the phenotype is determined by the chemokine receptor used by the virus for fusion and entry, either CCR5 or CXCR4 [1]. Cyclic V3 peptides bind to the corresponding co-receptors at micromolar concentrations [13,15]. A single Asp320→Arg mutation in a V3 peptide transformed it from an M-tropic to a T-tropic virus inhibitor [15]. These findings indicate that V3 contains a significant determinant directly interacting with the chemokine receptor regardless of the receptor type.

Residues Lys^{5P}, Ile^{7P} and Phe^{17P} of V3 are important for CCR5 utilization [44], and together with Ser^{6P} found to be important for the co-receptor choice [15], form a continuous surface in P1053 (Figure 4b). Arg^{15P}, also involved in CCR5 utilization [44], is separated from this patch by the sidechain of Arg^{8P}. Residue 320 of V3 is outside the epitope recognized by 0.5β. It is conceivable that in native V3, the sidechain of this residue, critical for the selection of the co-receptor type [15], is adjacent to the patch formed by Lys^{5P}, Ser^{6P}, Ile^{7P} and Phe^{17P}. It is noteworthy that a positively charged residue (usually lysine), an isoleucine, a positively charged residue (usually arginine) and a phenylalanine or another hydrophobic residue are highly conserved at gp120 positions corresponding to peptide residues 5, 7, 15 and 17, respectively [40].

The surface of V3 between the patch involved in co-receptor binding and the highly conserved GPG region contains variable residues. Gln^{10P} is part of a two-residue insertion appearing in only ~10% of all HIV-1 isolates. Arginine appears at position 8 only in ~11% of the HIV-1 isolates. Both Gln^{10P} and Arg^{8P} form large contact areas with the antibody surface as shown in Figure 5. The variability of these protruding residues in the gp120 molecule is probably responsible for the induction of strain-specific antibodies. These hot spots of variable residues very close to the conserved binding site for the chemokine receptors help the virus to evade the immune system.

The role of the GPG segment, the most conserved sequence in V3 [40], remains unclear. As this segment interacts with the antibody, it is most likely to be exposed in the gp120 molecule. In addition to what has been suggested previously [29], it is plausible that its function would be to stabilize the β-hairpin conformation by forming a reverse turn. Although the β hairpin was not observed for the MN strain [20–22], we previously suggested that it is common to most HIV-1 isolates [28,29]. A one-residue shift in the β turn in P1053 in comparison to MN peptides [29] and a formation of a six-residue rather than a four-residue loop accommodate the two-residue insertion that is typical of HIV-1_{IIIB} strain while conserving the location of the β strands within V3. The conformation of the turn in the GPGR sequence at the tip of the V3 peptide was found to be different in the HIV-1_{MN} and HIV-1_{IIIB} strains [29]. It is reasonable that the turn connecting the two β strands of P1053 influences the spatial orientation and exposure of the V3 sidechains interacting with the co-receptors and that of the highly variable residues that help the virus to escape from the immune system.

The peptide residues Val^{18P} and Thr^{19P} do not have any contacts with the antibody and, surprisingly, Ile^{9P} and Ala^{16P} have only minor contacts with 0.5β despite their location in a central region of the epitope (Figure 5). The involvement of Val^{18P}, Thr^{19P} and Ile^{9P} in many interactions within the bound peptide, the lack of interactions with the antibody and the hydrophobic character of Val^{18P} and Ile^{9P} suggest that they are buried in the free gp120 molecule.

Biological implications

The envelope glycoprotein of human immunodeficiency virus type-1 (HIV-1), consisting of an external domain, gp120, and a transmembrane domain, gp41, is the most important target for the humoral immune response that is elicited by an anti-HIV vaccine. The principal neutralizing determinant of gp120 is located within its third hypervariable region (V3 loop). Several HIV-1 V3 residues important for co-receptor choice were identified by examining naturally occurring mutants and using site-directed mutagenesis. Recently, several residues at the center of V3 were shown to be involved in chemokine receptor utilization. In a number of cases, anti-HIV antibodies inhibited V3–chemokine-receptor binding. The V3 loop was deleted from the gp120–CD4–antibody complex solved recently using X-ray crystallography. No direct structural information is therefore available on V3 and V3–antibody interactions.

The 0.5β antibody used in the present study was elicited against the gp120 molecule of the HIV-1_{IIIB} strain. Given that the whole gp120 was used as an immunogen, the interactions of 0.5β with the V3 peptide should serve as a reliable model for the interactions between the intact gp120 and anti-IIIB antibodies. Our nuclear magnetic resonance (NMR) results suggest that the surface of the V3 peptide in contact with the antibody is likely to correspond to a solvent-exposed region in the native

gp120 molecule. The conformation of the $V3_{IIIB}$ peptide bound to 0.5β consists of two antiparallel β strands linked by a QRGPGR (in single-letter amino acid code) loop. The solution structure of the 0.5β binding site in complex with P1053 provides insight into a component of the chemokine receptor-binding interaction with gp120. High-affinity binding of gp120 to the chemokine receptor probably involves V3 residues down-stream from the 0.5β epitope as well as residues in the conserved and occluded CD4i epitope. The highly variable and protruding residues next to the chemokine receptor binding site are likely to be included in the epitope recognized by antibodies against this site. Mutations in these variable residues limit the specificity of the neutralizing antibody and help the virus escape from the immune system.

The structure of the binding site of the anti-gp120 antibody in complex with the V3 peptide P1053 can be used to analyze the structural and functional implications of sequence variations on co-receptor usage and antibody specificity. This structure might help to construct a cocktail of V3 peptides that will induce a broadly neutralizing immune response. In the absence of the three-dimensional structure of the chemokine receptor involved in HIV-1 infection, the structure of V3 might be useful to design anti-HIV-1 drugs that target this receptor.

Materials and methods

Fv isotope labeling and sample preparation

The peptides were chemically synthesized on an Applied Biosystem 430A automated peptide synthesizer and purified by using high performance liquid chromatography (HPLC) as described elsewhere [26,27]. The 0.5β Fv was expressed in *E. coli* strain BL21(DE3) [45]. [U–^{13}C,^{15}N]-Fv was obtained using an efficient and cost-effective protocol. The cells were grown for 16 h at 37°C on 2xTY medium, containing glucose 1% (w/v), ampicillin (100 μg/ml) and chloramphenicol (25 μg/ml). The cell pellet was washed twice with 50 mM NaCl solution and then resuspended in isotope-enriched Celtone rich medium (Martek Biosciences Corp., US) supplemented with 0.5% ^{13}C-labeled glycerol. After incubation for 45 min at 30°C, induction was performed by adding 1 mM IPTG (isopropylthio-β-D-galactoside) followed by incubation for 16–18 h at 30°C. Next, 350 mM NaCl and a mixture of the following protease inhibitors were added to the cooled broth: aprotinin (2 μg/ml), EDTA (5 mM), leupeptin (2 μg/ml), pepstatin (1 μg/ml), PMSF (100 μg/ml), TPCK (100 μg/ml), benzoamidine (1 mM), iodoacetamide (1 mM) and *N*-ethylmaleimide (1 mM). This extensive use of protease inhibitors alleviated the problem of post-expression proteolysis of the correctly folded Fv. The Fv was purified on a set of three columns, including Sepharose CL-4B, DE-52 anion exchange, and an affinity column prepared with P1053 cross-linked to Sepharose CL-4B, and then additionally purified by HPLC on an Ultropac column (TSK G3000SWG) with a 250 mM phosphate elution buffer. A typical yield of ~10 mg of [U–^{15}N,^{13}C]-Fv per liter of Celtone medium was achieved.

The Fv–peptide complexes (27.6 kDa) were prepared by addition of a ~20% molar excess of lyophilized peptide to a dilute Fv solution (~0.05 mM), dialysis against 50 mM NH_4HCO_3 to remove peptide excess and lyophilization. Three samples of the 0.5β Fv–peptide complex were used: two 0.6 mM samples of [U–^{13}C,^{15}N]-Fv complexed with the unlabeled P1053 in H_2O (pH 7.1) and 0.75 mM [U–^{13}C,^{15}N]-Fv complexed with the unlabeled P1053 in D_2O (pD 7.2, uncorrected for the isotope effect). The samples contained 10 mM sodium phosphate buffer with 0.05% NaN_3 to prevent bacterial growth, and were placed in 5 mm Shigemi cells (Shigemi Inc., US).

NMR spectroscopy

All NMR spectra were recorded at 32°C on Bruker DRX800 and DMX600 spectrometers equipped with z-gradient triple-resonance probes and BTO temperature regulation units. The spectra were processed with NMRPipe/NMRDraw [46], and analyzed using the NMRView [47] program and in-house scripts. The following three-dimensional (3D) experiments were used to assign the Fv aliphatic sidechain resonances unassigned earlier: HBHA(CBCACO)NH [48], C(CO)NH [49], HACACO [50], HC(C)H-COSY [51] and HC(C)H-TOCSY (total correlation spectroscopy) [52]. Substantial chemical shift degeneracy of α-carbons in the ^{13}C-edited spectra could be partially resolved using 3D HBHA(CBCA)CO(CA)HA [53] and CBCACO(CA)HA [54] data sets. The assignment of aromatic sidechains was accomplished using 2D ^{13}C-TROSY [36], 3D (H)CCH-TROSY [36], Cβ(Cγ)CδHδ [37], and HC(C)H-TOCSY [52] optimized for aromatic sidechains. The following NOESY spectra were acquired: 3D NOESY-^{15}N-HSQC (heteronuclear single quantum correlation) with water flip-back and the use of radiation damping during the 80 ms mixing period [55–57], 3D NOESY-^{15}N-TROSY [58] with 34 and 84 ms mixing periods using Fv with selective chain labeling [34], 3D NOESY-^{13}C-HMQC (heteronuclear multiple quantum coherence spectroscopy) [59,60] in D_2O with a 76 ms mixing period, 3D NOESY-^{13}C-HMQC [59,60] with an 80 ms mixing period optimized for the aromatic sidechains, and 4D ^{13}C/^{13}C-separated NOESY [61] in D_2O with an 80 ms mixing period. A series of short ^{15}N-HSQC [62] spectra were used to identify slowly exchanging Fv amide protons.

In the 'BIRD-supplemented' NOESY spectra (see text), the heteronuclear one-bond couplings were allowed to evolve for the whole constant-time period (adjusted to slightly more than ~$1/^1J_{X-H}$ to ensure sufficient resolution in ^{1}H dimension) by simultaneous 180° pulses on ^{1}H and X channels. The constant-time t1 evolution compromised signal-to-noise of these spectra, but strong and medium NOEs originating from peptide protons could be observed. The unlabeled part of the antibody provides an attenuating (negative) component to positive NOEs originating from ^{13}C-bound protons. This BIRD-supplemented NOESY thus only complemented, but not substituted, conventional ^{13}C-edited spectra. Obviously, this approach is inapplicable for levels of isotopic enrichment much lower than those used in the present study, since ^{12}C-bound protons possess significantly longer T_2 values than ^{13}C-bound ones and can invert the peaks of a partially labeled component. The BIRD-supplemented ^{13}C-edited NOESY spectra were collected for the aliphatic and aromatic regions separately.

The quantitative J-spectroscopy approach [63] was employed to measure J couplings. The $^3J_{HNH\alpha}$ coupling constants were measured from 3D HNHA [64] experiments recorded for the Fv molecules with chain specific labeling [34] using water flip-back and an 18 ms dephasing period. The values of $^3J_{HNH\alpha}$ obtained from peak intensity ratios were scaled by a factor of 1.20 to account for fast spin-flips during the dephasing period. $^3J_{H\alpha H\beta}$ couplings were derived where possible from a 3D HACAHB [65] experiment recorded in D_2O. 2D HN(CG) and HN(CO)CG constant-time spin-echo difference experiments [66] were used to determine aromatic $^{13}C\gamma$–^{15}N and $^{13}C\gamma$–$^{13}C'J$ couplings, respectively. 2D spin-echo difference ^{13}C-HSQC spectra [67] were used to measure $^{13}C\gamma$–^{15}N and $^{13}C\gamma$–$^{13}C'$ J couplings of residues possessing γ-methyls.

Structure calculations

The X-PLOR 3.851 program [68] was used for structure calculations with standard simulated annealing protocols. All the peptide residues and the Fv CDR loops together with three N-terminal residues of both Fv chains (Asp^{1L}–Val^{3L}, Ser^{26L}–Met^{33L}, Tyr^{49L}–Asn^{53L}, Ser^{91L}–Phe^{96L},

Gln^{1H}–Gln^{3H}, Gly^{26H}–Glu^{35H}, Asn^{50H}–Asn^{58H}, Ile^{94H}–Tyr^{102H}) were allowed to move (26% of the whole Fv molecule), while the framework of 0.5β Fv was held fixed. The N termini of both VL and VH are in close spatial proximity to the CDRs of the Fv and were included in the calculations. The lists of constraints included the intermolecular constraint between the guanidinium group of Arg^{11P} and the carboxyl of Asp^{56H} from the previous mutational studies [30], and the ϕ and ψ dihedral constraints of Arg^{15P} derived from the solid-state NMR data [42]. The rest of the intra-peptide distance and dihedral restraints derived from isotope-filtering and isotope-editing studies [29] were used without changes. The structures of the bound P1053 [29] and the 0.5β Fv model were used as the starting coordinates. After simulated annealing calculations, the structures were minimized using 800-step Powell minimization with full Lennard–Jones potential representation and the electrostatic term included. An NOE force constant of 50 kcal/mole was used throughout the calculations. R^{-6} distance averaging for degenerate atoms was employed. The NOE cut-off for acceptable structures was set to 0.4 Å. The calculated structures were analyzed for covalent geometry and NOE violations with Aqua/Procheck-NMR [69] and MOLMOL [70] programs and displayed with InsightII (MSI Corp., US).

Accession numbers

Coordinates of the average minimized 0.5β Fv–P1053 complex structure were deposited in the Brookhaven Protein Data Bank with accession code 1nqz.

Acknowledgements

We thank Frank Delaglio (NIH, Bethesda, MD) for NMR processing software, Ad Bax (NIH, Bethesda, MD) and Stephan Grzesiek (Basel University Biozentrum, Switzerland) for pulse sequences and continuous assistance in the project. We are indebted to Fred Naider (CUNY, NY) for fruitful discussions, to Eva Meirovitch (Bar-Ilan University, Israel) for time on the DMX600 spectrometer and to Jordan Chill (Weizmann Institute) for careful reading of the manuscript. Gabriel Faiman and Amnon Horovitz (Weizmann Institute) are acknowledged for the joint effort to establish the Fv expression system. This research was supported by the NIH grant GM53329, the Minerva Foundation and the Israel Academy of Sciences. JA is Joseph and Ruth Owades Professor in Chemistry.

References

1. Berger, E.A. *et al.*, & Sodroski, J. (1998). A new classification for HIV-1. *Nature* **391**, 240.
2. Alkhatib, G. *et al.*, & Berger, E.A. (1996). CC CKR5: a RANTES, MIP-1α, MIP-1β receptor as a fusion cofactor for macrophage-tropic HIV-1. *Science* **272**, 1955-1958.
3. Choe, H. *et al.*, & Sodrosky, J. (1996). The β-chemokine receptors CCR3 and CCR5 facilitate infection by primary HIV-1 isolates. *Cell* **85**, 1135-1148.
4. Deng, H. *et al.*, & Landau, N.R. (1996). Identification of a major co-receptor for primary isolates of HIV-1. *Nature* **381**, 661-666.
5. Doranz, B.J. *et al.*, & Doms, R.W. (1996). A dual-tropic primary HIV-1 isolate that uses fusin and the β-chemokine receptors CKR-5, CKR-3 and CKR-2b as fusion cofactors. *Cell* **85**, 1149-1158.
6. Dragic, T. *et al.*, & Paxton, W.A. (1996). HIV-1 entry into CD4 cells is mediated by the chemokine receptor CC-CKR-5. *Nature* **381**, 667-673.
7. Feng, Y., Broder, C.C., Kennedy, P.E. & Berger, E.A. (1996). HIV-1 entry cofactor: functional cDNA cloning of a seven-transmembrane, G protein-coupled receptor. *Science* **272**, 872-877.
8. Rusche, J.R. *et al.*, & Matthews, T.J. (1988). Antibodies that inhibit fusion of human immunodeficiency virus-infected cells bind a 24-amino acid sequence of the viral envelope, gp120. *Proc. Natl Acad. Sci. USA* **85**, 3198-3202.
9. Wu, L. *et al.*, & Sodroski, J. (1996). CD4-induced interaction of primary HIV-1 gp120 glycoproteins with the chemokine receptor CCR-5. *Nature* **384**, 179-183.
10. Trkola, A. *et al.*, & Moore, J.P. (1996). CD4-dependent, antibody-sensitive interactions between HIV-1 and its co-receptor CCR-5. *Nature* **384**, 184-187.
11. Cocchi, F. *et al.*, & Lusso, P. (1996). The V3 domain of the HIV-1 gp120 envelope glycoprotein is critical for chemokine mediated blockade of infection. *Nat. Med.* **2**, 1244-1247.
12. Rabehi, L., Seddiki, N., Benjouad, A., Gluckman, J.C. & Gattegno, L. (1998). Interaction of human immunodeficiency virus type 1 envelope glycoprotein V3 loop with CCR5 and CD4 at the membrane of human primary macrophages. *AIDS Res. Hum. Retroviruses* **14**, 1605-1615.
13. Xiao, X. *et al.*, & Dimitrov, D.S. (1999). Constitutive cell surface association between CD4 and CCR5. *Proc. Natl Acad. Sci. USA* **96**, 7496-7501.
14. Sakaida, H. *et al.*, & Uchiyama, T. (1998). T-tropic human immunodeficiency virus type 1 (HIV-1)-derived V3 loop peptides directly bind to CXCR-4 and inhibit T-tropic HIV-1 infection. *J. Virol.* **72**, 9763-9770.
15. Verrier, F., Borman, A.M., Brand, D. & Girard, M. (1999). Role of the HIV type 1 glycoprotein 120 V3 loop in determining co-receptor usage. *AIDS Res. Hum. Retroviruses* **15**, 731-743.
16. Rizzuto, C.D. *et al.*, & Sodroski, J. (1998). A conserved HIV gp120 glycoprotein structure involved in chemokine receptor binding. *Science* **280**, 1949-1953.
17. Matthews, T.J. (1994). Tenth anniversary perspectives on AIDS. *AIDS Res. Hum. Retroviruses* **10**, 631-632.
18. Moore, J.P. *et al.*, & Ho, D.D. (1995). Primary isolates of human immunodeficiency virus type 1 are relatively resistant to neutralization by monoclonal antibodies to gp120, and their neutralization is not predicted by studies with monomeric gp120. *J. Virol.* **69**, 101-109.
19. VanCott, T.C., Polonis, V.R., Loomis, L.D., Michael, N.L., Nara, P.L. & Birx, D.L. (1995). Differential role of V3-specific antibodies in neutralization assays involving primary and laboratory-adapted isolates of HIV type 1. *AIDS Res. Hum. Retroviruses* **11**, 1379-1391.
20. Rini, J.M., Stanfield, R.L., Stura, E.A., Salinas, P.A., Profy, A.T. & Wilson, I.A. (1993). Crystal structure of a human immunodeficiency virus type 1 neutralizing antibody, 50.1, in complex with its V3 loop peptide antigen. *Proc. Natl Acad. Sci. USA* **90**, 6325-6329.
21. Ghiara, J.B., Stura, E.A., Stanfield, R.L., Profy, A.T. & Wilson, I.A. (1994). Crystal structure of the principal neutralization site of HIV-1. *Science* **264**, 82-85.
22. Stanfield, R.L., Cabezas, E., Satterthwait, A., Stura, E., Profy, A. & Wilson, I. (1999). Dual conformations for the HIV-1 gp120 V3 loop in complexes with different neutralizing Fabs. *Structure* **7**, 131-142.
23. Kwong, P.D., Wyatt, R., Robinson, J., Sweet, R.W., Sodroski, J. & Hendrickson, W.A. (1998). Structure of an HIV gp120 envelope glycoprotein in complex with the CD4 receptor and a neutralizing human antibody. *Nature* **393**, 648-659.
24. Matsushita, S. *et al.*, & Putney, S. (1988). Characterization of a human immunodeficiency virus neutralizing monoclonal antibody and mapping of the neutralizing epitope. *J. Virol.* **62**, 2107-2114.
25. Skinner, M.A., *et al.*, & Matthews, T.J. (1988). Characteristics of a neutralizing monoclonal antibody to the HIV envelope glycoprotein. *Aids Res. Hum. Retroviruses* **4**, 187-197.
26. Zvi, A., Hiller, R. & Anglister, J. (1992). Solution conformation of a peptide corresponding to the principal neutralizing determinant of $HIV\text{-}1_{IIIB}$: a two-dimensional NMR study. *Biochemistry* **31**, 6972-6979.
27. Zvi, A., *et al.*, & Anglister, J. (1995). Mapping of the antigenic determinant recognized by an anti-gp120 HIV neutralizing antibody by two-dimensional NMR. *Eur. J. Biochem.* **229**, 178-187.
28. Zvi, A., Feigelson, D.J., Hayek ,Y. & Anglister, J. (1997). The conformation of the principal neutralizing determinant of HIV-1 in complex with an anti-gp120 HIV-neutralizing antibody studied by 2D-NMR difference spectroscopy. *Biochemistry* **36**, 8619-8627.
29. Tugarinov, V., Zvi, A., Levy, R. & Anglister, J. (1999). A *cis* proline turn linking two β-hairpin strands in the solution structure of an antibody-bound $HIV\text{-}1_{IIIB}$ V3 peptide. *Nat. Struct. Biol.* **6**, 331-335.
30. Zvi, A., Tugarinov, V., Faiman G.A., Horovitz, A. & Anglister, J. (2000). A model of a gp120 V3 peptide in complex with an HIV-neutralizing antibody based on NMR and mutant cycle constraints. *Eur. J. Biochem.* **267**, 767-779.
31. Chothia, C. & Lesk, A.M. (1987). Canonical structures for the hypervariable regions of immunoglobulins. *J. Mol. Biol.* **19**, 901-917.
32. Chothia, C., *et al.*, & Poljak, R.J. (1989). Conformations of immunoglobulin hypervariable regions. *Nature* **342**, 877-883.
33. Givol, D. (1991). The minimal antigen binding fragment of antibodies-the Fv fragment. *Mol. Immunol.* **28**, 1379-1367.
34. Tugarinov, V., Levy, R., Dahan-Shokoroy, A. & Anglister, J. (1999). Backbone and C^{β} assignments of the anti-gp120 antibody Fv fragment complexed with an antigenic peptide. *J. Biomol. NMR.* **13**, 193-194.
35. Pervushin, K., Riek, R., Wider, G. & Wüthrich, K. (1997). Attenuated T_2 relaxation by mutual cancellation of dipole–dipole coupling and chemical shift anisotropy indicates an avenue to NMR structures of very large biological macromolecules. *Proc. Natl Acad. Sci. USA* **94**, 12366-12371.
36. Pervushin, K., Riek, R., Wider, G. & Wüthrich, K. (1998). Transverse

relaxation-optimized spectroscopy (TROSY) for NMR studies of aromatic spin systems in ^{13}C-labeled proteins. *J. Am. Chem. Soc.* **120**, 6394-6400.
37. Yamazaki, T., Forman-Kay, J.D. & Kay, L.E. (1993). Two-dimensional NMR experiments for correlating $^{13}C^{\beta}$ and $^{1}H^{\delta/\varepsilon}$ chemical shifts of aromatic residues in ^{13}C-labeled proteins via scalar couplings. *J. Am. Chem. Soc.* **115**, 11054-11055.
38. Sheriff, S. *et al.*, & Davies, D.R. (1987). Three-dimensional structure of an antibody–antigen complex. *Proc. Natl Acad. Sci. USA* **84**, 8075-8079.
39. Garbow, J.R., Weitekamp, D.P. & Pines, A.(1982). BIRD-bilinear rotation decoupling. *Chem. Phys. Lett.* **93**, 514-518.
40. LaRosa, G.J. *et al.*, & Putney, S.D. (1990) Conserved sequence and structural elements in the HIV-1 principal neutralizing determinant. *Science* **249**, 932-935.
41. Morea, V., Tramontano, A., Rustici, M., Chothia, C. & Lesk, A.M. (1998). Conformations of the third hypervariable region in the VH domain of immunoglobulins. *J. Mol. Biol.* **275**, 269-294.
42. Weliky, D.P, Bennett, A.E., Zvi, A., Anglister, J., Steinbach, P.J. & Tycko, R. (1999). Solid-state NMR evidence for an antibody-dependent conformation of the V3 loop of HIV-1 gp120. *Nat. Struct. Biol.* **6**, 141-145.
43. De Jong, J-J., De Ronde, A., Keulen, W., Tersmette, M. & Goudsmit, J. (1992). Minimal requirements for the human immunodeficiency virus type 1 V3 domain to support the syncytium-inducing phenotype: analysis by single amino acid substitution. *J. Virol.* **66**, 6777-6780.
44. Wang, W-K., Dudek, T., Essex, M. & Lee, T-H. (1999). Hypervariable region 3 residues of HIV type 1 gp120 involved in CCR5 coreceptor utilization: therapeutic and prophylactic implications. *Proc. Natl Acad. Sci. USA* **96**, 4558-4562.
45. Faiman, G., Levy, R., Anglister, J. & Horovitz, A. (1996). Contribution of arginine residues in the RP135 derived from the V3 loop of gp120 to its interaction with the Fv fragment of the 0.5β HIV-1 neutralizing antibody. *J. Biol. Chem.* **271**, 13829-13833.
46. Delaglio, F., Grzesiek, S., Vuister, G. W., Zhu, G., Pfeifer, J. & Bax, A. (1995). NMRPipe: a multidimensional spectral processing system based on UNIX pipes. *J. Biomol. NMR* **6**, 277-293.
47. Johnson, B.A. & Blevins, R.A. (1994). NMRView: a computer program for the visualization and analysis of NMR data. *J. Biomol. NMR* **4**, 603-614.
48. Grzesiek, S. & Bax, A. (1993). Amino acid type determination in the sequential assignment procedure of uniformly ^{13}C/^{15}N enriched proteins. *J. Biomol. NMR* **3**, 185-204.
49. Grzesiek, S., Anglister, J. & Bax, A. (1993). Correlation of backbone amide and aliphatic sidechain resonances in ^{13}C/^{15}N-enriched proteins by isotropic mixing of ^{13}C magnetization. *J. Magn. Reson. Series B* **101**, 114-119.
50. Grzesiek, S. & Bax. A. (1993). The origin and removal of artifacts in 3D HCACO spectra of proteins uniformly enriched with ^{13}C. *J. Magn. Reson. Series B* **102**, 103-106.
51. Bax A., Clore, G.M., Driscoll, P.C., Gronenborn, A.M., Ikura, M. & Kay, L.E. (1990). Practical aspects of proton–carbon–carbon–proton three-dimensional correlation spectroscopy of ^{13}C-labeled proteins. *J. Magn. Reson.* **87**, 620-627.
52. Bax. A., Clore, G.M. & Gronenborn, A.M. (1990). ^{1}H–^{1}H correlation via isotropic mixing of ^{13}C magnetization: a new three-dimensional approach for assigning ^{1}H and ^{13}C spectra of ^{13}C-enriched proteins. *J. Magn. Reson.* **88**, 425-431.
53. Kay, L.E. (1993). A three-dimensional NMR experiment for the separation of aliphatic carbon chemical shifts via the carbonyl chemical shift in ^{15}N, ^{13}C-labeled proteins. *J. Magn. Reson. Series B* **101**, 110-113.
54. Kay, L.E. (1993). Pulsed-field gradient-enhanced three-dimensional NMR experiment for correlating $^{13}C^{\alpha/\beta}$, ^{13}C', and $^{1}H^{\alpha}$ chemical shifts in uniformly ^{13}C-labeled proteins dissolved in H_2O. *J. Am. Chem. Soc.* **115**, 2055-2057.
55. Marion, D., Kay, L.E., Sparks, S.W., Torchia, D.A. & Bax, A. (1989). Three-dimensional heteronuclear NMR of ^{15}N-labeled proteins. *J. Am. Chem. Soc.* **111**, 1515-1517.
56. Grzesiek, S. & Bax, A. (1993). The importance of not saturating water in protein NMR. Application to sensitivity enhancement and NOE measurements. *J. Am. Chem. Soc.* **115**, 12593-12594.
57. Lippens, G., Dhalluin, C. & Wieruszeski, J.M. (1995). Use of a water flip-back pulse in homonuclear NOESY. *J. Biomol. NMR* **5**, 327-331.
58. Zhu, G., Kong, X. & Sze, K. (1999). Gradient-enhanced TROSY NOE spectroscopy. *J. Biomol. NMR* **13**, 77-81.
59. Ikura, M., Kay, L.E. & Bax, A. (1990). Three-dimensional NOESY-HMQC spectroscopy of a ^{13}C-labeled protein. *J. Magn. Reson.* **86**, 204-209.
60. Zuiderweg, E.R.P., McIntosh, L.P., Dahlquist, F.W. & Fesik, S.W. (1990). Three-dimensional ^{13}C-resolved proton NOE spectroscopy of uniformly ^{13}C-labeled proteins for the NMR assignment and structure determination of larger molecules. *J. Magn. Reson.* **86**, 21-216.
61. Clore, G.M. & Gronenborn, A.M. (1991). Structures of larger proteins in solution:three- and four-dimensional heteronuclear NMR spectroscopy. *Science* **252**, 1390-1999.
62. Bodenhausen, G. & Ruben, D.J. (1980). Natural abundance nitrogen-15 NMR by enhanced heteronuclear spectroscopy. *Chem. Phys. Lett.* **69**, 185-188.
63. Bax, A. *et al.* & Vuister, G.W. (1994). Measurement of homo- and heteronuclear J-couplings from quantitative J-correlation. *Methods Enzymol.* **239**, 79-105.
64. Kuboniwa, H., Grzesiek, S., Delaglio, F. & Bax, A. (1994). Measurement of H^{N}–H^{α} J-couplings in calcium-free calmodulin using new 2D and 3D water-flip-back methods. *J. Biomol. NMR* **4**, 871-878.
65. Grzesiek, S., Kuboniwa, H., Hinck, A.P. & Bax, A. (1995). Multiple-quantum line-narrowing for the measurement of H^{α}–H^{β} J-couplings in isotopically labeled proteins. *J. Am. Chem. Soc.* **117**, 5312-5315.
66. Hu, J.S., Grzesiek, S. & Bax, A. (1997). Two-dimensional NMR methods for determining χ^1 angles of aromatic residues in proteins from three-bond $J_{C'C\gamma}$ and $J_{NC\gamma}$ couplings. *J. Am. Chem. Soc.* **119**, 1803-1804.
67. Vuister, G.W., Wang, A.C. & Bax, A. (1993). Measurement of three-bond nitrogen-carbon J couplings in proteins uniformly enriched in nitrogen-15 and carbon-13. *J. Am. Chem. Soc.* **115**, 5334-5335.
68. Brünger, A.T. (1993). *XPLOR Version 3.1. A System for X-ray Crystallography and NMR.* (Yale University Press, New Haven, CT).
69. Laskowsky, R.A., Rullman, J.A.C., MacArthur, M.W., Kaptein, R. & Thornton, J.M. (1996). AQUA and PROCHECK-NMR: programs for checking the quality of protein structures solved by NMR. *J. Biomol. NMR* **8**, 477-486.
70. Koradi, R., Billeter, M. & Wüthrich, K. (1996). MOLMOL: a program for display and analysis of macromolecular structures. *J. Mol. Graphics* **14**, 51-55.
71. Al-Lazikani, B., Lesk, A.M. & Chothia, C. (1997). Standard conformations for the canonical structures of immunoglobulins. *J. Mol. Biol.* **273**, 927-948.

Because *Structure with Folding & Design* operates a 'Continuous Publication System' for Research Papers, this paper has been published on the internet before being printed (accessed from http://biomednet.com/cbiology/str). For further information, see the explanation on the contents page.